ISSN 0006-2979, Biochemistry (Moscow), 2010, Vol. 75, No. 1, pp. 25-35. © Pleiades Publishing, Ltd., 2010.
Original Russian Text © O. A. Smitienko, M. N. Mozgovaya, I. V. Shelaev, F. E. Gostev, T. B. Feldman, V. A. Nadtochenko, O. M. Sarkisov, M. A. Ostrovsky, 2010, published in Biokhimiya, 2010, Vol. 75, No. 1, pp. 34-45.
Originally published in Biochemistry (Moscow) On-Line Papers in Press, as Manuscript BM09-105, December 20, 2009.

Femtosecond Formation Dynamics of Primary Photoproducts of Visual Pigment Rhodopsin

O. A. Smitienko[1], M. N. Mozgovaya[1]*, I. V. Shelaev[2], F. E. Gostev[2], T. B. Feldman[1], V. A. Nadtochenko[2,3], O. M. Sarkisov[2], and M. A. Ostrovsky[1]

[1]*Emanuel Institute of Biochemical Physics, Russian Academy of Sciences, ul. Kosygina 4, 119334 Moscow, Russia; fax: (495) 135-4101; E-mail: ibcp@sky.chph.ras.ru; mozgovaya.mariya@gmail.com*
[2]*Semenov Institute of Chemical Physics, Russian Academy of Sciences, ul. Kosygina 4, 119991 Moscow, Russia; fax: (495) 651-2191; E-mail: icp@chph.ras.ru*
[3]*Institute of Problems of Chemical Physics, Russian Academy of Sciences, pr. Akademika Semenova 1, 142432 Chernogolovka, Moscow Region, Russia; fax: (496) 522-5636*

Received April 1, 2009
Revision received June 8, 2009

Abstract—The coherent 11-*cis*-retinal photoisomerization dynamics in bovine rhodopsin was studied by femtosecond time-resolved laser absorption spectroscopy at 30-fs resolution. Femtosecond pulses of 500, 535, and 560 nm wavelength were used for rhodopsin excitation to produce different initial Franck–Condon states and relevant distinct values of the vibrational energy of the molecule in its electron excited state. Time evolution of the photoinduced rhodopsin absorption spectra was monitored after femtosecond excitation in the spectral range of 400-720 nm. Oscillations of the time-resolved absorption signals of rhodopsin photoproducts represented by photorhodopsin$_{570}$ with vibrationally-excited all-*trans*-retinal and rhodopsin$_{498}$ in its initial state with vibrationally-excited 11-*cis*-retinal were studied. These oscillations reflect the dynamics of coherent vibrational wave-packets in the ground state of photoproducts. Fourier analysis of these oscillatory components has revealed frequencies, amplitudes, and initial phases of different vibrational modes, along which the motion of wave-packets of both photoproducts occurs. The main vibrational modes established are 62, 160 cm^{-1} and 44, 142 cm^{-1} for photorhodopsin$_{570}$ and for rhodopsin$_{498}$, respectively. These vibrational modes are directly involved in the coherent reaction under the study, and their amplitudes in the power spectrum obtained through the Fourier transform of the kinetic curves depend on the excitation wavelength of rhodopsin.

DOI: 10.1134/S0006297910010049

Key words: rhodopsin, photorhodopsin, bathorhodopsin, femtosecond time-resolved laser absorption spectroscopy, coherent reaction, wave-packet

The retinal-containing visual pigment rhodopsin (R_{498}) is one of the earliest proteins of the animal kingdom; it appeared in the Precambrian about 580-550 million years ago [1]. The chromophore center of this protein is highly conserved, and chromophore photoisomerization as a trigger of the phototransduction process is a general reaction in all species ranging from the most primitive (phototaxis) to highly organized (vision). The visual pigment rhodopsin is a typical member of the G-protein-coupled receptor family. Its molecule is composed of chromophore (11-*cis*-retinal) and protein (opsin). The 11-*cis*-retinal chromophore is covalently attached to the apoprotein opsin through a protonated Schiff-base linkage to the ε-amino group of Lys296. Absorption of a photon results in isomerization of 11-*cis*-retinal to the all-*trans* configuration. This reaction, in turn, induces conformational changes in opsin with breakage of the covalent bond between retinal and opsin (photolysis). The phototransduction process starts at the stage of formation of metarhodopsin II leading to an electrical signal in the photoreceptor cell.

Isomerization of 11-*cis*-retinal chromophore of the rhodopsin molecule to the all-*trans* form is the first and the only photochemical reaction in the complex process

Abbreviations: batho$_{535}$, bathorhodopsin; FC, Franck–Condon; HTG, *n*-nonyl-β-D-heptylthioglucoside; PES, potential energy surface; photo$_{570}$, photorhodopsin; R_{498}, rhodopsin; ROS, rod outer segments.

* To whom correspondence should be addressed.

of phototransduction. This reaction can be considered as unique in its features. First, it is a fast photochemical reaction. Its duration is less than 200 fs [2-4], whereas the photoisomerization of free retinal in solution takes several picoseconds [5]. Second, it goes with high quantum yield of 0.65 [6], whereas the quantum yield of free retinal photoisomerization in a solution does not exceed 0.15 [7]. Third, most of the energy of the absorbed photon (more than 60%) is transformed to the chemical energy of conformational changes of the protein [8]. This is indicative of a crucial role of the protein environment in dynamics of this reaction.

The study of photoisomerization of rhodopsin containing 11-*cis*-retinal or its analogs with totally or partially blocked C_{11}=C_{12} double bond has led to the conclusion that the photoisomerization occurs in the excited state and finalizes with the transition of the molecule to its ground state to form the first reaction product, phototorhodopsin ($photo_{570}$), which converts to the next product, bathorhodopsin ($batho_{535}$) [2, 3, 9, 10]. Inspection of kinetics curves describing the formation of the reaction primary products within the femto- and picosecond time ranges has revealed coherent phenomena associated with the phase motion of retinal nuclei in the reaction process – with coherent vibrational wave packets [2, 11, 12]. The dependence of both the reaction quantum yield and maximum of rhodopsin fluorescence band on the excitation wavelength was detected in experiments on stationary photolysis [6, 13].

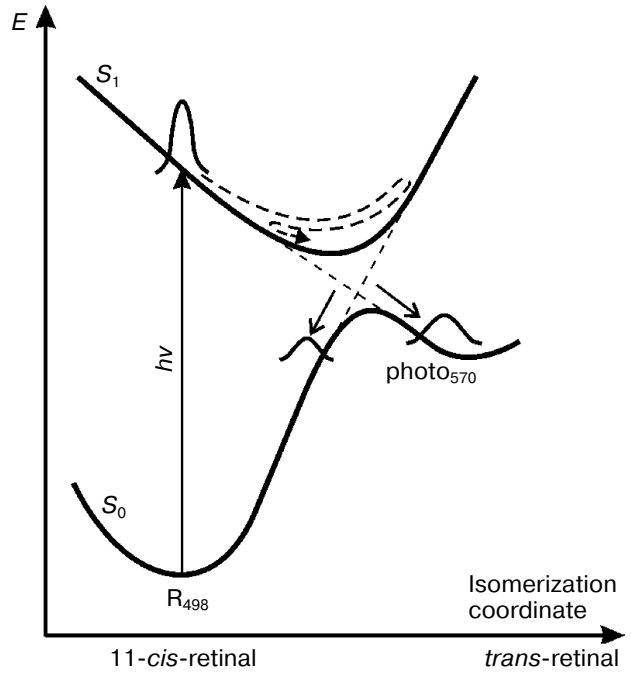

Fig. 1. Scheme of potential energy surfaces participating in primary reactions of rhodopsin.

Thus, all the regarded features of the photochemical reaction of 11-*cis*-retinal *cis-trans* isomerization in rhodopsin lead to the conclusion that, the $S_1 \rightarrow S_0$ transition to the ground state is faster than the equilibrium achievement between the vibrational degrees of freedom in the S_1 electron excited state. This fact can explain experimentally observed dependence of quantum yield on the excitation wavelength.

The study on *cis-trans* isomerization of the retinal using the laser femtosecond spectroscopy technique has demonstrated that a femtosecond pulse coherently excites a superposition of the chromophore vibrational states on S_1 excited potential energy surface (PES). This set of the excited vibrational states is called coherent vibrational wave packet (hereinafter referred to as "wave packet") (Fig. 1). The wave packet migrates along the S_1 PES from the initial Franck–Condon (FC) state to the region of S_0/S_1 conical intersection of PESs [12, 14-16]. The transition from the S_1 to the S_0 PES is most likely in a vicinity of the intersection point. This transition corresponds to formation of the initial product, hypothetically $photo_{570}$. The $S_1 \rightarrow S_0$ transition in the vicinity of conical intersection is frequently accompanied by the maintenance of the wave packet on the S_0 surface, that is, the reaction flows in coherent mode [17]. An important sign of such reaction mode is coherent oscillations observed in the dynamics of reagent decay and product formation. The observation of oscillations in kinetics curves by the method of femtosecond spectroscopy is not sufficient for making a conclusion on coherent mode. The wave packets observable might not be associated with degrees of freedom determining the unit process of the reaction, and these wave packets are inactive in relation to the unit. This circumstance is taken into account when the question of coherent mode is analyzed in the present work.

Determination of vibrational modes belonging to the active reaction modes is one of the most important goals when elucidating the reaction mechanism. It is now supposed that these reaction vibrational modes are low-frequency vibrations of the polyene retinal chain (<600 cm^{-1}), which have mostly delocalized torsion character, as well as high-frequency out-of-plane oscillations of hydrogen atoms of the C_{11}=C_{12} bond (~970 cm^{-1}) [18-21]. In spite of the fact that the set of frequencies for normal vibrations of 11-*cis*-retinal in rhodopsin and the character of corresponding movements have been determined [18-20], the question remains unsolved concerning which of these vibrations participate in the photoisomerization reaction, and what is the extent of the participation.

The question concerning the influence of the initial excitation energy of rhodopsin on the dynamics of retinal isomerization and on the dynamics of non-radiative $S_1 \rightarrow S_0$ transition of the molecule has not been studied in detail. We studied earlier the features of the 11-*cis*-retinal photoisomerization reaction in rhodopsin after excitation by 308 nm pulses near the absorption β-band of the visu-

al pigment molecule [22]. Under this excitation of rhodopsin the transmission of photoexcitation energy was shown to occur from the S_n high electron excited states of retinal to the S_1 state with the representative time of about 100 fs. Following this, the processes possessing the same time characteristics flow in rhodopsin, which are identical to those occurring after its excitation with visible light in its main absorption α-band (~450-600 nm).

The tasks of the work included the study of differential spectra of rhodopsin absorption after the excitation with femtosecond pulse at various energies of the excitation quantum leading to the emergence of different initial FC states of the system, analysis of the oscillatory effects in time-resolved absorption signals of the reaction products, determination of amplitude and phase–frequency characteristics of wave packets formed at various excitation wavelengths (500, 535, and 560 nm), as well as to reveal torsion vibrational frequencies of the rhodopsin chromophore carbons belonging to the reaction vibrational modes.

MATERIALS AND METHODS

Rhodopsin preparation. Rod outer segments (ROS) from bovine (*Bos taurus*) retinas and rhodopsin extracts were prepared by the modified method of Okada et al. [23]. Retinas were isolated no later than 3 h after slaughtering, and then 53% sucrose solution (Sigma, USA) in the buffer A (10 mM Mops (Sigma, Germany), pH 7.5, containing 30 mM NaCl (Sigma, USA), 60 mM KCl (Sigma, USA), 2 mM $MgCl_2$ (Sigma, Japan), 0.1 mM phenylmethylsulfonyl fluoride (PMSF) (Sigma, China), 1 mM dithiothreitol (Sigma, China), and 0.01% NaN_3 (Sigma, China)) was added to the retina preparations, 1 ml per each retina. The suspension was vigorously shaken for 3 min and centrifuged for 40 min at 2000*g*. The supernatant was diluted four times with buffer A and centrifuged for 60 min at 2000*g*. The pellet was resuspended in 25 ml of 40% sucrose in buffer A, and then 10 ml of the buffer A was layered on top to make a stepwise gradient of density with following centrifugation for 60 min at 4°C and 25,000*g* on a Beckman Coulter Avanti J30I centrifuge equipped with JS 24,38 rotor. The ROS fraction was sampled at the buffer–sucrose border, diluted with buffer B (5 mM Tris-HCl (Fluka, Germany), pH 8.0, containing 0.5 mM $MgCl_2$, 0.4 mM EDTA (Sigma, USA), 1 mM dithiothreitol, and 0.01% NaN_3) to the density of 1.05 g/cm^3, and the absorption spectrum of the resulting suspension was recorded. Absorption spectra were recorded using a Shimadzu UV-1700 (Japan) spectrophotometer. ROS were precipitated by centrifugation for 30 min at 41,400*g*. The pellet was resuspended in 0.01% NaN_3 in distilled water and centrifuged for 30 min at 41,400*g*. The pellet, consisting of photoreceptor membrane disks, was frozen at –80°C.

To prepare rhodopsin extracts, the disks were thawed and resuspended in 1.6% *n*-nonyl-β-D-heptylthioglucoside (*n*-heptyl-β-D-thioglucoside) (HTG) (Anatrace, USA) detergent in buffer C (0.1 M CH_3COONa (Fluka, Germany), 0.1 M $(CH_3COO)_2Zn$ (Fluka, Germany), 0.3 M ammonium sulfate (Sigma, USA), and 0.01% NaN_3, pH 6.0), 0.8 ml of the solution per mg rhodopsin. The extract was incubated for 3 h at 20°C and then 12 h at 4°C. The rhodopsin extract was centrifuged for 30 min at 41,400*g* followed by filtration through a Millipore filter (Millex GS PVDF 0.22 μm) and concentrated using Millipore centrifuge filters (Amicon Ultra-4 Ultracell 30k). Thus prepared rhodopsin HTG-extracts had concentration of 4-5 mg/ml and possessed A_{280}/A_{500} = 1.7-1.9 purity. A 2 M solution of NH_2OH (Fluka, Switzerland) was added to the final concentration of 0.1 M before measurements. All the manipulations with samples containing rhodopsin were carried out under dim red illumination.

Femtosecond laser spectroscopy. The absorption femtosecond laser spectroscopy studies were carried out using the equipment described earlier [24] by the method of excitation-probing. Femtosecond pulses were generated in a Tsunami (Spectra Physics, USA) solid-state titanium-sapphire laser (τ = 80 fs, E = 0.8 nJ, λ = 802 nm, f = 80 MHz) with pumping by continuous emission of a MilleniaVs (Spectra Physics) solid-state laser with diode pumping (λ = 530 nm, P = 4.65 W). Femtosecond pulses with parameters τ = 90 fs, E = 1.2 mJ, λ = 805 nm, and f = 1 kHz were produced after the amplification in a Spitfire (Spectra Physics) regenerative amplifier with pumping by Evolution X (Spectra Physics) laser emission (P = 8 W, λ = 527 nm, f = 1 kHz, τ = 150 ns).

To produce exciting and probing pulses, the amplified emission was divided into two beams. One beam designed for the production of exiting pulses was directed to the delay line allowing delay of the exciting pulse relatively the probing one in 0-600 ps range with minimum step of 3.3 fs. The laser pulse was directed thereafter to a non-collinear optical parametric amplifier (Clark MXR, Germany), which transformed the 805 nm wavelength into λ = 500, 535, and 560 nm wavelengths (τ = 20-30 fs, E = 70, 130, and 200 nJ, respectively). Different energies of exciting pulses were chosen to achieve equal concentrations of excited states. The second beam of the amplified laser emission was attenuated to the energy of ~0.5-2 μJ and focused to a cell with water in which the supercontinuum pulse was generated with the spectral range of 400-1000 nm and total energy less than 10 nJ. The produced supercontinuum pulse was divided into two channels: probing and reference pulses. The signals were registered using an SP-300 (Acton, USA) polychromator and SPEC-10 (Roper Scientific, USA) CCD-camera.

The experiments were carried out at room temperature in a flow cell of 0.5 mm thickness. Fifty spectra were accumulated at each delay time between exciting and

probing pulses. Due to the light scattering associated with the exciting pulse passing, the regions 495-535, 500-560, and 540-600 nm were inaccessible for probing in the experiments with the exciting pulses of 500, 535, and 560 nm, respectively. In control experiments, the measurements were done in detergent solution without rhodopsin (1.6% HTG solution in the buffer C) and the absence of interfering effects of the detergent or buffer was demonstrated. A coherent response of nonlinear optical polarization of the solvent repeating the shape of the exciting pulse typical of the femtosecond photolysis was only observed in the time ranges of the exciting pulse action. The experimental data were processed with Span software (Shareware: Belousov, Verzakov), written using the Matlab computer language medium, and Igor Pro software.

RESULTS AND DISCUSSION

Femtosecond laser spectroscopy of 11-*cis*-retinal photoisomerization in rhodopsin. Change in the photoinduced absorption of the visual pigment recorded after the excitation of the molecule with pulses of 500, 535, and 560 nm is demonstrated as differential spectra (Fig. 2) and kinetic curves (Figs. 3 and 4).

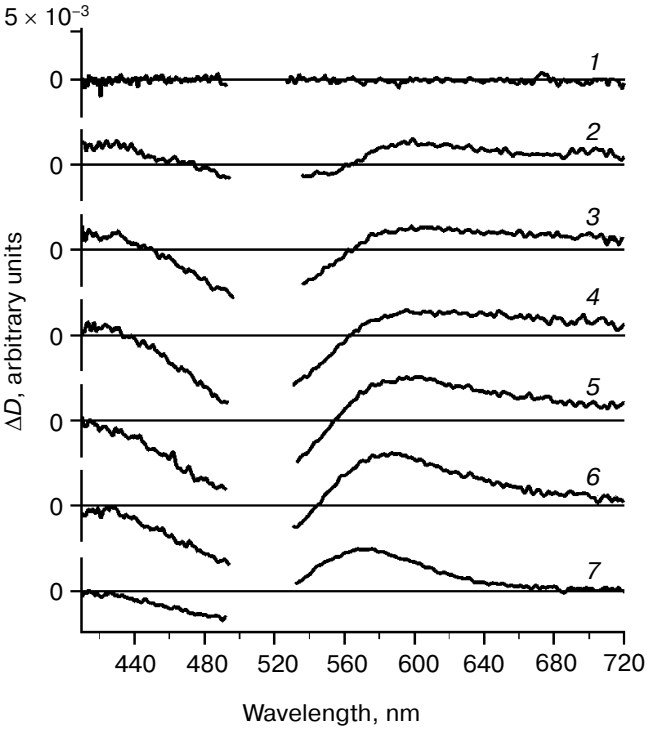

Fig. 2. Spectra of photoinduced absorption of rhodopsin recorded after excitation of rhodopsin extract with 500 nm pulses in 410-720 nm spectral range at the following delay times: –0.11 (*1*), 0.06 (*2*), 0.08 (*3*), 0.1 (*4*), 0.15 (*5*), 0.2 (*6*), and 3 ps (*7*).

The differential spectrum (Fig. 2) represents the difference between the sample absorption after its excitation and that of the non-excited sample. Generally, the differential absorption spectrum is expressed as follows:

$$\Delta D = D(\mathrm{ESA}) + D(\mathrm{GSA}) - D_0(\mathrm{GSA}) - D(\mathrm{SE}),$$

where D(ESA) is the absorption of rhodopsin excited state, D(GSA) is the sum of absorption of the rhodopsin ground state after the excitation and the isomerization reaction products photo$_{570}$ and batho$_{535}$, D_0(GSA) is the absorption of R_{498} ground state before the excitation, and $-D$(SE) is a possible stimulated emission from the excited state. The difference D(GSA) – D_0(GSA) ignoring absorption of the isomerization reaction products is the bleaching of the R_{498} ground state and is due to depletion of the population of this state due to the excitation. The signal D(SE) was not observed in the given system within the studied spectral range of 400-720 nm.

The positive absorption associated with the formation of photo$_{570}$, the first reaction product of retinal isomerization, is observed 60 fs after the excitation at 600 nm (Fig. 2). This absorption reaches its maximum at 200 fs (Fig. 3; curves *6* and *7*) and shifts to shorter wavelength after 2-3 ps, reflecting the transition of photo$_{570}$ to the next product, batho$_{535}$.

The negative absorption band associated with R_{498} bleaching increases in the 440-560 nm region approximately 150 fs after the excitation (Fig. 2). However, the R_{498} bleaching band must arise within the exciting pulse time frames ~30 fs. This apparent contradiction is explainable by the contribution of the D(ESA) rhodopsin excited state to the absorption within this spectral region with the maximum about 500-510 nm at early delay times [2, 3]. The formation of photo$_{570}$ likely occurs from this electron excited state. Besides, we observed some positive absorption within 410-460 nm region at early times (Figs. 2 and 3), which is probably a shoulder of the absorption band attributed to the rhodopsin excited state. This absorption is observable earlier than 40 fs and disappears in ~150 fs after the excitation (Fig. 3; curve *1*). Thus, one can say that the decay of the signal within 410-560 nm range in 40-150 fs time range reflects the disappearance of rhodopsin excited state, which is in agreement with the time of photo$_{570}$ formation.

The negative absorption band at 500 nm begins decreasing after its maximum to 130-150 fs, but this process is not monoexponential. In our opinion, the reduction of this negative band is due to the returning of one-third of rhodopsin molecules to the S_0 initial state of R_{498} and, to a lesser extent, due to formation of photo$_{570}$ and batho$_{535}$ products, which also contributes to the absorption within this spectral region (Fig. 3; curves *2-5*).

A positive absorption band is observed in the 650-720 nm region at the delay times up to 2 ps (Figs. 2 and

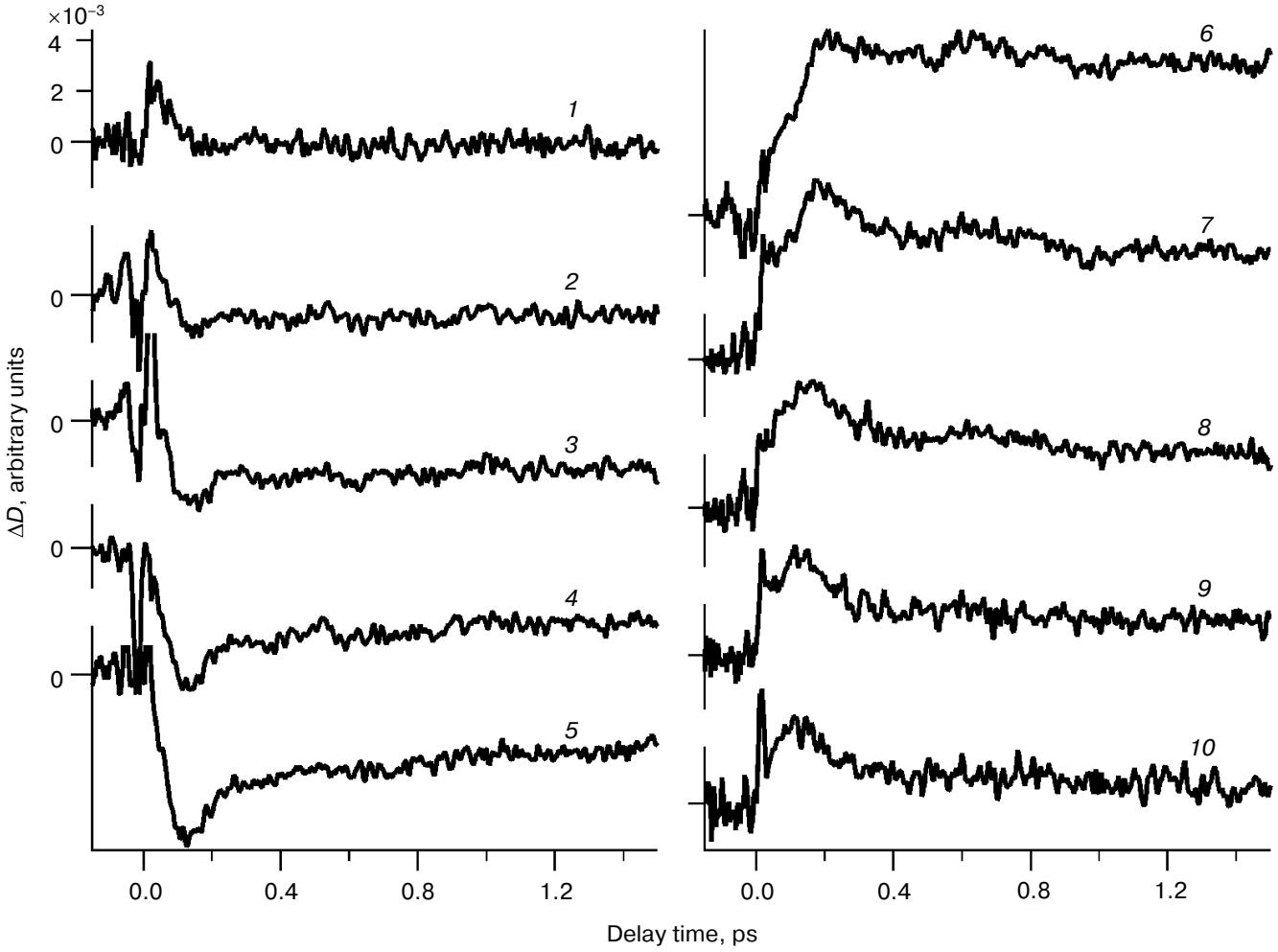

Fig. 3. Kinetic curves of photoinduced rhodopsin absorption changes recorded upon excitation of rhodopsin extracts with 535 nm pulses at delay times of –0.2-to-1.5 ps at probing wavelengths of 420 (*1*), 440 (*2*), 460 (*3*), 480 (*4*), 500 (*5*), 580 (*6*), 610 (*7*), 640 (*8*), 670 (*9*), and 690 nm (*10*). The signal from control detergent solution was subtracted from the kinetic curves. The sharp transient on kinetic curves at zero time is due to the coherent spike.

3), which arises approximately in ~100 fs after the excitation and disappears with representative times of 60 fs and 1 ps (Fig. 3; curve *10*). The absorption in this region was observed earlier [4] and was attributed to rhodopsin excited state, from which some molecules return to the R_{498} initial state S_0. Kinetics of the long-wavelength absorption band disappearance does not correspond to the formation of $photo_{570}$ (Figs. 2 and 3). Thus, this excited state can be associated with the process of the R_{498} initial state formation requiring a time longer than 200 fs.

Analysis of kinetic curves. Kinetics curves and spectra of rhodopsin photoinduced absorption recorded after rhodopsin excitation with 500, 535, and 560 nm pulses within the 410-650 nm spectral region in the 0.09-11 ps time range, can be interpreted using the following simplified kinetic model (see Scheme) describing the transitions shown in Fig. 1.

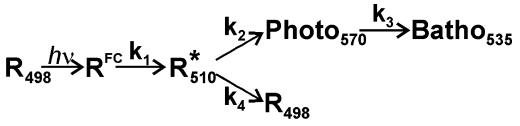

Kinetic scheme of sequence of rhodopsin phototransformations

R^{FC} designates the initial (FC) state in this model, and R^*_{510} designates the electron excited state with the absorption maximum at 510 nm. The model does not reflect the wave packet oscillation dynamics and is used for simplified procedure of estimation of the transition times. As we show below, this model facilitates demonstration of the oscillation component in kinetic curves on the background of relaxation components of the process. Based on the Scheme, one can solve the system of differential equations for $[R_{498}]$, $[R^{FC}]$, $[R^*_{510}]$, $[photo_{570}]$, and

[batho$_{535}$] (concentrations of all the participants of the reaction) using equation

$$k_4 = k_2\left(\frac{1-\varphi}{\varphi}\right),$$

where φ is the quantum yield of the isomerization reaction (φ ~ 0.65 [6]). The following equation describes the change in optical density taking into account the solution of the equation system for the Scheme:

$$\Delta D(t) = a_0 + a_1\exp(-t/\tau_1) + a_2\exp(-t/\tau_2) + a_3\exp(-t/\tau_3),$$

$$\tau_1 = \frac{1}{k_1}, \quad \tau_2 = \frac{1}{k_2+k_4} = \frac{\varphi}{k_2}, \quad \tau_3 = \frac{1}{k_3}. \qquad (1)$$

An example of model curves of type (1) is given in Fig. 4. The chosen wavelengths for probing are typical for the bleaching spectrum range and partial regeneration of the initial rhodopsin state R_{498} (Fig. 4; 480 nm) and for the region of the photo$_{570}$ and batho$_{535}$ formation (Fig. 4; 610 nm). The construction of model curves of type (1) allows determination of time constants characterizing the kinetics of primary reactions of rhodopsin after the excitation with pulses within the 500-560 nm wavelength range. The time constants were 40 fs for the formation of rhodopsin excited state R^*_{510}, 110-125 fs for photoexcitation energy transition from the R^*_{510} to the photo$_{570}$ potential well, 2.4-2.65 ps for the transition of photo$_{570}$ to batho$_{535}$, and 175-230 fs for the transition from the excited state R^*_{510} to the ground state R_{498} of rhodopsin. The time constant values obtained from the analysis are virtually the same (within the confidence interval) to those obtained from experiments with rhodopsin excitation with 500, 535, and 560 nm pulses. Nevertheless, some

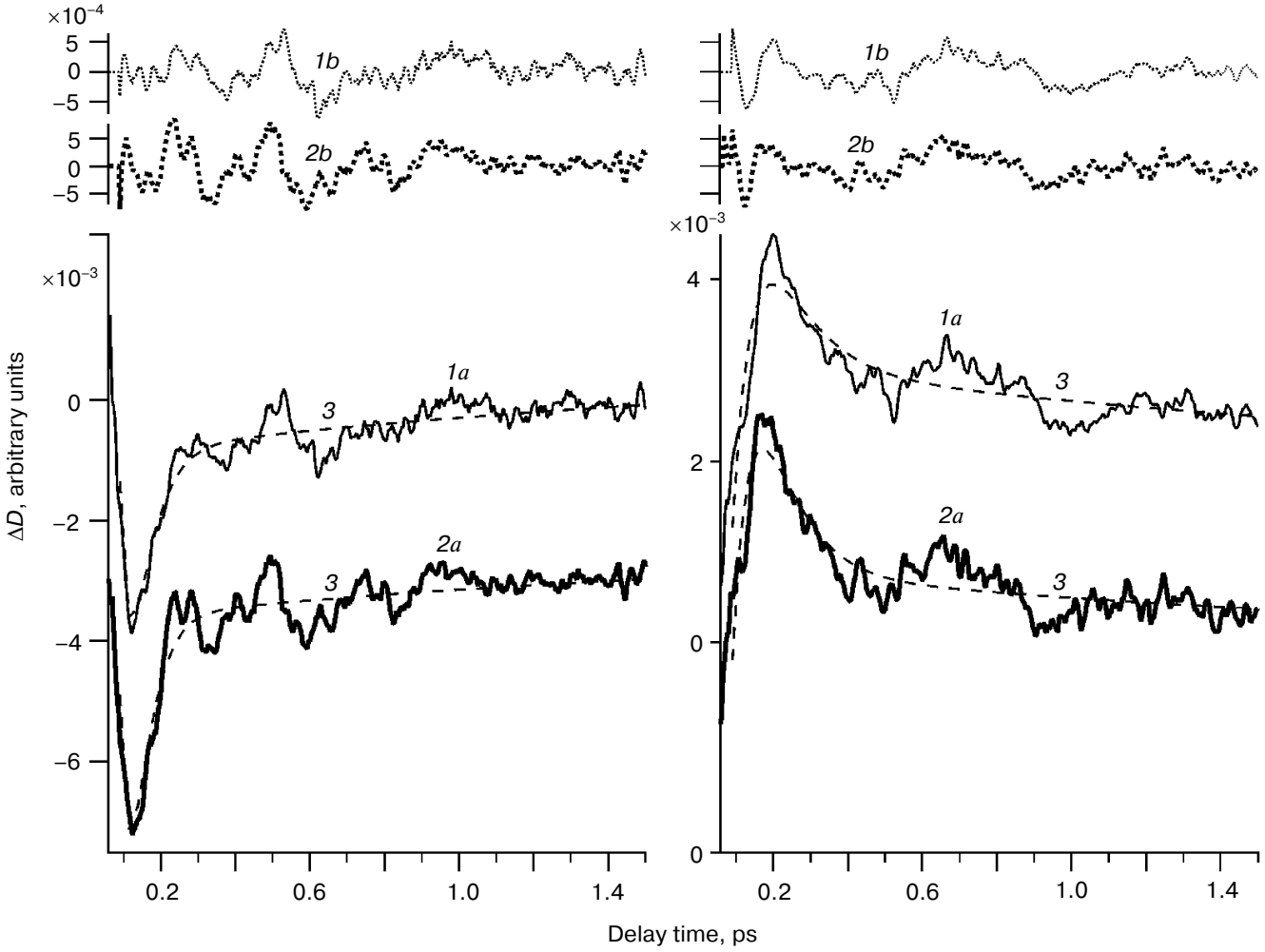

Fig. 4. Comparison of non-normalized kinetic curves for rhodopsin photoinduced absorption recorded after excitation with 500 nm (*1a*) and 560 nm (*2a*) pulses at delay times of 0.06-1.5 ps and 480 nm (left) and 610 nm (right) probing wavelengths. The figure also shows model curves (*3*) and oscillatory components of the kinetic curves (*1b*, *2b*).

difference is observed in the character of kinetic curves obtained in the experiments on rhodopsin excitation with 500, 535, and 560 nm pulses at times up to a few picoseconds.

As we mentioned above, the photochemical isomerization of 11-*cis*-retinal in rhodopsin demonstrates the features of a coherent reaction. Oscillations of signal associated with the formation of wave packets (Figs. 3 and 4) are observed in the kinetic curves describing the formation of the photoisomerization products, photo$_{570}$ and batho$_{535}$, as well as the formation of the R_{498} molecule. The oscillations are observed at times up to 2 ps. Since this time is less than batho$_{535}$ formation time, it is possible that oscillations of signal are associated more likely with photo$_{570}$ time-resolved absorption. Note, that no signal oscillation is observed in the kinetic curves reflecting the absorption of two excited states of rhodopsin (Fig. 3; curves *1* and *10*).

The system of differential equations corresponding to the Scheme and its solution (Eq. (1)) do not take into account the oscillatory components of the signal. The oscillatory components are represented in the upper part of Fig. 4 for the kinetic curves given in this figure. These curves were obtained by subtraction of the model curves from the experimental kinetic curves. Thus, one can suppose that the difference in kinetic curves observed at the times of existence of wave packets is due to formation of different FC states after rhodopsin excitation by pulses of various wavelengths and different wave packet dynamics in the course of the reaction.

Oscillations of time-resolved signals of primary photoproduct absorption were discovered earlier in photoinduced signals of rhodopsin absorption, as well as in emission signals of bacteriorhodopsin and protonated Schiff bases of retinal within the time range up to several picoseconds [11, 12, 25]. The presence of oscillations reflects the fact that the photoreaction in all the mentioned systems has many common features and its course is non-adiabatic as a result of coherent motion of the nuclear system along the reaction coordinate.

The signal oscillations characterize the motion of wave packets along the S_0 PES of the reaction product, and the analysis of the oscillation frequency components can give information on oscillatory modes contributing to the corresponding wave packets. The contribution of each frequency component can be evidence for the role of a distinct vibrational mode in the process of photo$_{570}$ and R_{498} formation. Therefore, Fourier analysis was carried out for oscillatory components of the kinetic curves, the results being presented in Fig. 5. Power spectra for the Fourier components obtained within the absorption ranges of R_{498} are represented in Fig. 5 (a-c) and power spectra obtained within the absorption ranges of photo$_{570}$ and batho$_{535}$ in Fig. 5 (d-f).

The identical set of frequencies was obtained over all the R_{498} absorption band (420-540 nm) with the following values: 44, 89, 142, ~191, ~240, and ~315 cm^{-1}, with dominating frequencies at 142 cm^{-1} and, to a lesser extent, at 44 cm^{-1}. The identical set of frequencies was obtained within the absorption band of photo$_{570}$ (540-650 nm), but with higher values: 62, ~115, 160, 204, ~244, ~280, ~320, ~360, ~430, and ~470 cm^{-1} with dominating frequencies at 62 cm^{-1} and, to a lesser extent, at 160 cm^{-1}.

Oscillations with frequencies near to 62 and 142 cm^{-1} in fast rhodopsin photoinduced signals were observed earlier [2, 11]. The revealed oscillation frequencies are in agreement with the frequencies of vibrational modes obtained for rhodopsin by Raman spectroscopy [20] and picosecond time-resolved Raman spectroscopy [26]. The frequencies of vibrational modes of rhodopsin ground state were determined using these methods, for instance, 93, 131, 246, 260, 320, 410, 446, and 568 cm^{-1} and for the products photo$_{570}$ (batho$_{535}$), for instance, 167, 244, 300 (320), 401, and 503 cm^{-1} (Stokes frequencies) and 282, 350, and 477 cm^{-1} (anti-Stokes frequencies). Types of retinal molecule movements in rhodopsin corresponding to the observed frequencies were determined as well. For instance, the 260 cm^{-1} frequency was attributed to torsional vibrations of the C_{10}-C_{13} region, 246 cm^{-1} to C–C–C bends, and 93, 131, and 320 cm^{-1} to delocalized torsional vibrations of the retinal molecule. One can suppose that the main vibrational modes observed in the present work, namely 44, 62, 142, and 160 cm^{-1}, correspond to the delocalized torsional vibrations of the polyene retinal chain [18, 20].

Since dependence on phase of nuclear vibrational motion is a feature of coherent processes, the analysis of change in the vibration phase with distinct frequencies in the reaction flow indicates the involvement of corresponding vibrational modes in the reaction and coherent character of the reaction course itself. With this goal, the oscillation phases were determined with the main observed frequencies (44, 62, 142, and 160 cm^{-1}) through the whole probing range (Fig. 6).

The analysis demonstrated that the phase of all studied oscillation frequencies does not depend on probing wavelength in the region of R_{498} absorption and the region of photo$_{570}$ absorption; however, the phase sharply changes almost by 180° on the transition between these spectral regions (~520-540 nm). This effect unambiguously indicates that, within the region of S_0/S_1 PES conical intersection, the transition from the excited state to the products (photo$_{570}$ and batho$_{535}$) and to the initial state R_{498} occurs in the mode of coherent nuclear vibrations, which is characteristic of a wave packet. In other words, the wave packet motion along the reaction coordinate, which takes place in the course of coherent reaction, should be reflected in the phase shift of the reaction vibrational modes if two different wave packets passed through the conical intersection at different times (Fig. 1).

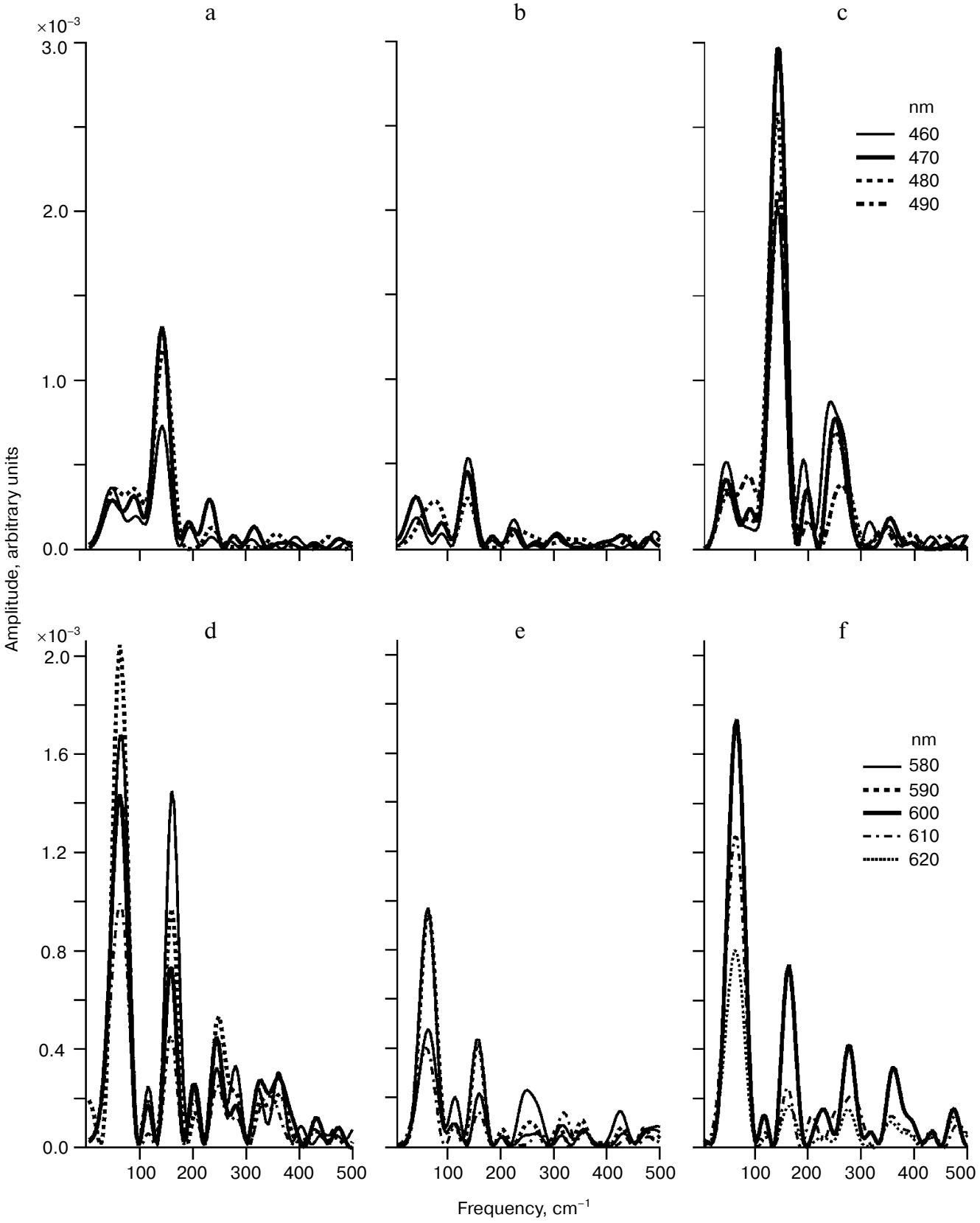

Fig. 5. Power spectra for the Fourier components of oscillations of the rhodopsin photoinduced absorption kinetic curves obtained after excitation with 500 (a, d), 535 (b, e), and 560 nm (c, f) pulses within 0.09-1 ps time range at 460-490 nm (a-c) and 580-620 nm (d-f) probing wavelengths.

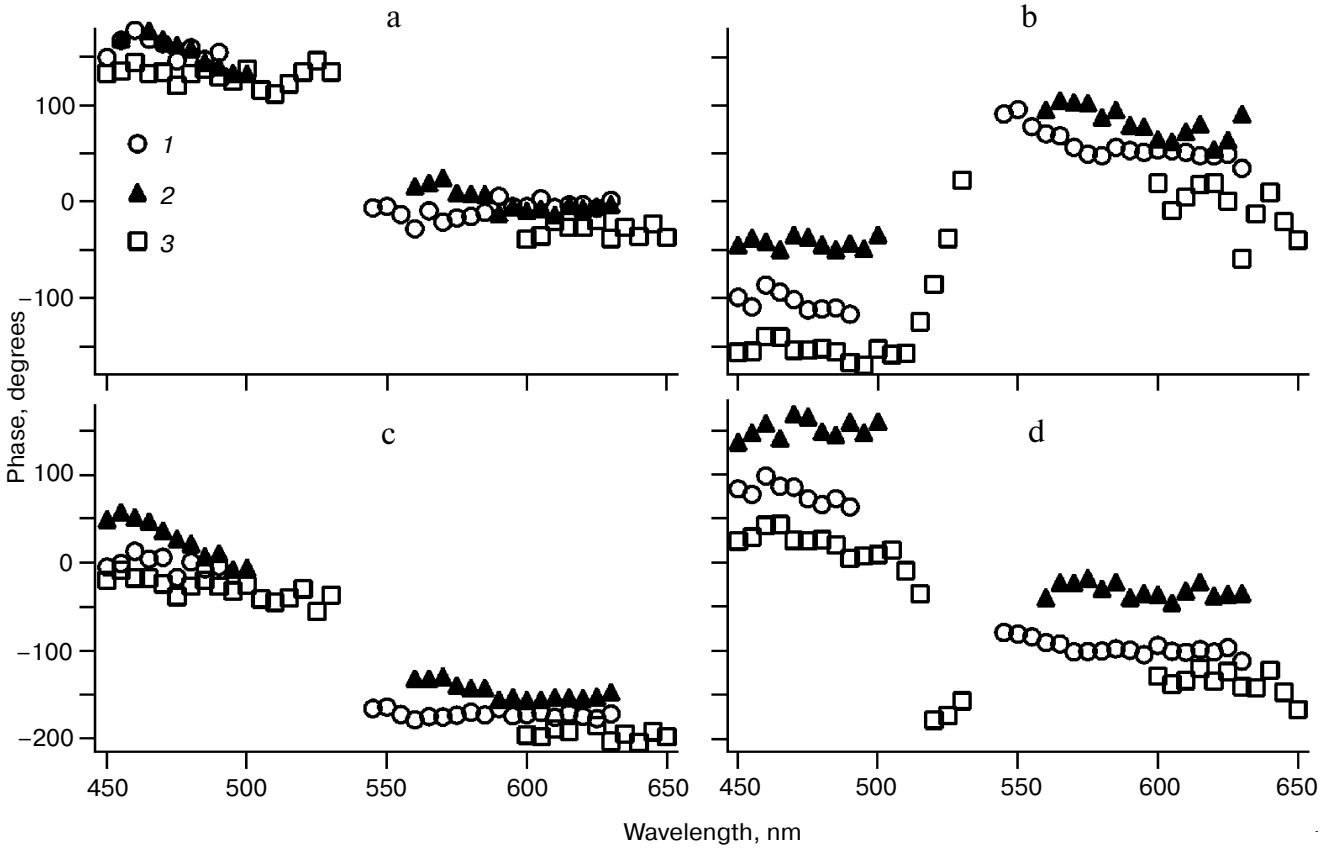

Fig. 6. Dependence of phases of the main observed oscillation frequencies 44 (a), 142 (b), 62 (c), and 160 cm^{-1} (d) on probing wavelength for experiments with rhodopsin excitation by 500 (*1*), 535 (*2*), and 560 nm (*3*) pulses.

Thus, the oscillation frequencies (44, 62, 142, and 160 cm^{-1}) revealed in the present work correspond to the vibrational modes that are active both in the elementary act of 11-*cis*-retinal isomerization in rhodopsin and in recovery of the R_{498} ground state.

$Photo_{570}$ and R_{498} formed due to the photoexcitation energy transition to the ground state possess a large storage of vibrational energy. The disappearance dynamics of oscillations of time-resolved absorption signals from these products reflects the redistribution process of vibrational energy between different modes. In the case of $photo_{570}$, this process corresponds to the transition of this product to the next product, $batho_{535}$, whose formation finalizes accumulation of 60% of the absorbed light quantum energy in the rhodopsin molecule. Characteristic fall times for the oscillation components with frequencies of 44, 62, 142, and 160 cm^{-1} were determined to estimate the times required for redistribution of the vibrational energy in $photo_{570}$ and R_{498} products. The oscillation components of rhodopsin photoinduced absorption signals regarded within the 90-3000 fs time range and the 460-490 and 580-620 nm spectral ranges were described by the following function:

$$F(t) = \sum_j b_j \exp\left(-\frac{t}{\tau_j}\right)\sin(\varphi_j + \omega_j t), \qquad (2)$$

where b_j is the contribution to the signal from the j oscillation component with phase φ_j and frequency ω_j; and τ_j is the fall time of the j component. Characteristic fall times obtained from the construction of model curves of type (2) are presented in the table.

As it can be seen from the table, the fall times of oscillation with frequencies of 62 and 160 cm^{-1} are longer than those with frequencies of 44 and 142 cm^{-1} and do not depend on rhodopsin excitation wavelength within the confidence interval. Thus, we conclude that the formation of $photo_{570}$ and its transition to $batho_{535}$ are accompanied by longer-lived oscillations, as compared with those featuring the return of the molecule to the ground state R_{498}. This suggests a longer time of coherency (lifetime of wave packet) for modes directly implicated in photoisomerization because it is physiologically important to enhance quantum yield of this process in comparison with the process of return of the molecule to the ground state R_{498}. Probably the protein surrounding

Characteristic fall times of oscillations (ps) with frequencies f (cm^{-1}) within absorption regions of R_{498} (460-490 nm) and $photo_{570}$ (580-620 nm) after excitation of rhodopsin with pulses λ (nm)

λ	R_{498}		$Photo_{570}$	
	f = 44	142	62	160
500	0.21 ± 0.04	0.48 ± 0.09	1.04 ± 0.16	0.68 ± 0.13
560	0.19 ± 0.03	0.48 ± 0.05	0.78 ± 0.11	0.71 ± 0.30

the retinal plays an important role in keeping the coherency on reaction vibrational modes by hindering the vibration relaxation process for distinct vibrational modes. As can be seen from the table, the fall times of the main oscillations with frequencies of 62 and 160 cm^{-1} reflecting redistribution processes of vibration energy and vibrational relaxation in $photo_{570}$ to $batho_{535}$ transition are within 1 ps limits, whereas the time of $batho_{535}$ formation was estimated as 2.5 ps. This fact suggests that most processes in which the rhodopsin molecule looses excessive vibrational energy flow with the active participation of other higher-frequency vibrational modes. Data that can serve as a confirmation of this fact were obtained in work [26], where the times of disappearance of anti-Stokes frequencies (>282 cm^{-1}) were estimated in picosecond time-resolved Raman spectra and comprised 2.0-2.7 ps, which is typical for $photo_{570}$ product.

When rhodopsin was excited by pulses with various wavelengths within the 500-560 nm range, virtually identical oscillation frequencies of kinetic curves (Fig. 5), frequency phases of 44 and 62 cm^{-1} (Fig. 6), and frequency fall times of 44, 62, 144, and 160 cm^{-1} were obtained, whereas Fourier analysis demonstrated that change in the excitation photon energy by 2000 cm^{-1} influences both the amplitude ratio of different Fourier components (Fig. 5) and their phases (Fig. 6). When supposing that this amplitude change is due to energy redistribution in different vibrational modes taking into account the coherent character of the reaction, one can qualitatively explain the experimental data of work [6] on the dependence of the reaction quantum yield on the excitation wavelength within the 500-570 nm range.

Thus, the results are indicative of the dependence of wave packet dynamics during the photoisomerization of 11-*cis*-retinal in rhodopsin on the characteristics of the initial FC state and reflect different trajectories of motion of wave packets. Frequencies, amplitudes, and phases of vibrational modes participating in the photochemical reaction of 11-*cis*-retinal isomerization in the rhodopsin molecule were revealed in the present work. The data confirm a hypothesis put forward earlier [19, 20], which states that delocalized low-frequency torsional vibrations of the chromophore polyene chain play a crucial role in 11-*cis*-retinal photoisomerization in rhodopsin.

The change in energy of excitation photon by 2000 cm^{-1} has been demonstrated to alter the amplitude ratio of different reacting vibrational modes at constancy of their frequencies. These data confirm non-statistical coherent character of the photoreaction of the rhodopsin molecule and reveal a possibility for realization of coherent control of the reaction product yield via directed change of phase characteristics of wave packets corresponding to distinct vibrational modes. So, for instance, the photoisomerization reaction quantum yield can be changed, as demonstrated in work [27] on bacteriorhodopsin as an example, through the alteration of phase–amplitude characteristics of spectral components of the excitation pulse. The approach developed in the present work can serve as an experimental criterion for coherency in other reactions, along with photoisomerization of 11-*cis*-retinal in opsin chromophore center, and as a method for determination of activity of various vibrational modes.

This study was supported by the Russian Academy of Sciences Presidium Program of Fundamental Studies "Theoretical and Experimental Studies on the Nature of the Chemical Bond and Mechanisms of the Most Important Chemical Reactions and Processes" (Program 1 of the Department of Chemistry and Material Science of the Russian Academy of Sciences) and by the Russian Foundation for Basic Research grants (Nos. 08-04-00200 and 08-03-00728).

REFERENCES

1. Lamb, T. D., Collin, S. P., and Pugh, E. N. (2007) *Nat. Rev. Neurosci.*, **8**, 960-976.
2. Schoenlein, R. W., Peteanu, L. A., Mathies, R. A., and Shank, C. V. (1991) *Science. New Ser.*, **254**, 412-415.
3. Peteanu, L. A., Schoenlein, R. W., Wang, Q., Mathies, R. A., and Shank, C. V. (1993) *Proc. Natl. Acad. Sci. USA*, **90**, 11762-11766.
4. Haran, G., Morlino, E. A., Matthes, J., Callender, R. H., and Hochstrasser, R. M. J. (1999) *Phys. Chem. A*, **103**, 2202-2207.
5. Kandori, H., Katsuta, Y., Msayoshi, I., and Sasabe, H. (1995) *J. Am. Chem. Soc.*, **117**, 2669-2670.

6. Kim, J. E., Tauber, M. J., and Mathies, R. A. (2001) *Biochemistry*, **40**, 13774-13778.
7. Koyama, Y., Kubo, K., Komori, M., Yasuda, H., and Mukai, Y. (1991) *Photochem. Photobiol.*, **54**, 433-443.
8. Cooper, A. (1979) *Nature*, **282**, 531-533.
9. Shichida, Y., Matuoka, S., and Yoshizawa, T. (1984) *Photobiochem. Photobiophys.*, **7**, 221-228.
10. Mizukami, T., Kandori, H., Shichida, Y., Chen, A.-H., Derguini, F., Caldwell, C. G., Bigge, C., Nakanishi, K., and Yoshizawa, T. (1993) *Proc. Natl. Acad. Sci. USA*, **90**, 4072-4076.
11. Wang, Q., Schoenlein, R. W., Peteanu, L. A., Mathies, R. A., and Shank, C. V. (1994) *Science*, *New Ser.*, **266**, 422-424.
12. Smitienko, O. A., Shelaev, I. V., Gostev, F. E., Fel'dman, T. B., Nadtochenko, V. A., Sarkisov, O. M., and Ostrovsky, M. A. (2008) *Dokl. RAN*, **421**, 1-5.
13. Kochendoerfer, G. G., and Mathies, R. A. (1996) *J. Phys. Chem.*, **100**, 14526-14532.
14. Garavelli, M., Celani, P., Bernardi, F., Robb, M. A., and Olivucci, M. (1997) *J. Am. Chem. Soc.*, **119**, 6891-6901.
15. Garavelli, M., Vreven, T., Celani, P., Bernardi, F., Robb, M. A., and Olivucci, M. (1998) *J. Am. Chem. Soc.*, **120**, 1285-1288.
16. Gonzalez-Luque, R., Garavelli, M., Bernardi, F., Merchan, M., Robb, M. A., and Olivucci, M. (2000) *Proc. Natl. Acad. Sci. USA*, **97**, 9379-9384.
17. Worth, G. A., and Cederbaum, L. S. (2004) *Annu. Rev. Phys. Chem.*, **55**, 127-158.
18. Hudson, B. S., Kohler, B. E., and Schulten, K. (1982) in *Excited States* (Lim, E. C., ed.) Vol. 6, Academic Press, N. Y., pp. 1-95.
19. Loppnow, G. R., and Mathies, R. A. (1988) *Biophys. J.*, **54**, 35-43.
20. Lin, S. W., Groesbeek, M., van der Hoef, I., Verdegem, P., Lugtenburg, J., and Mathies, R. A. (1998) *J. Phys. Chem. B*, **102**, 2787-2806.
21. Kukura, P., McCamant, D. W., Yoon, S., Wandschneider, D. B., and Mathies, R. A. (2005) *Science*, **310**, 1006-1009.
22. Antipin, S. A., Fel'dman, T. B., Gostev, F. E., Smitienko, O. A., Sarkisov, O. M., and Ostrovsky, M. A. (2004) *Dokl. RAN*, **396**, 105-108.
23. Okada, T., Takeda, K., and Kouyama, T. (1998) *Photochem. Photobiol.*, **67**, 495-499.
24. Shelaev, I. V., Gostev, F. E., Nadtochenko, V. A., Shkuropatov, A. Ya., Zabelin, A. A., Mamedov, M. D., Semenov, A. Yu., Sarkisov, O. M., and Shuvalov, V. A. (2008) *Photosynth. Res.*, **98**, 95-103.
25. Hou, B., Friedman, N., Ottolenghi, M., Sheves, M., and Ruhman, S. (2003) *Chem. Phys. Lett.*, **381**, 549-555.
26. Kim, J. E., and Mathies, R. A. (2002) *J. Phys. Chem. A*, **106**, 8508-8515.
27. Prokhorenko, V. I., Nagy, A. M., Waschuk, S. A., Brown, L. S., Birge, R. R., and Miller, R. J. D. (2006) *Science*, **313**, 1257-1261.